Available online at www.sciencedirect.com
ScienceDirect
Infrared Physics & Technology 50 (2007) 182–186
INFRARED PHYSICS & TECHNOLOGY
www.elsevier.com/locate/infrared

NIR, MWIR and LWIR quantum well infrared photodetector using interband and intersubband transitions

Fabio Durante P. Alves [a,*], G. Karunasiri [b], N. Hanson [b], M. Byloos [c], H.C. Liu [c], A. Bezinger [c], M. Buchanan [c]

[a] Instituto Tecnologico de Aeronautica (ITA), Praca Marechal Eduardo Gomes, 50, Vila das Acacias, CEP 12228-900, Sao Jose dos Campos, SP, Brazil
[b] Department of Physics, Naval Postgraduate School, Monterey, CA 93943, USA
[c] Institute for Microstructural Sciences, National Research Council, Ottawa, Canada K1A 0R6

Available online 17 November 2006

Abstract

This paper presents the design, fabrication and characterization of a QWIP photodetector capable of detecting simultaneously infrared radiation within near infrared (NIR), mid wavelength infrared (MWIR) and long wavelength infrared (LWIR). The NIR detection was achieved using interband transition while MWIR and LWIR were based on intersubband transition in the conduction band. The quantum well structure was designed using a computational tool developed to solve self-consistently the Schrödinger–Poisson equation with the help of the shooting method. Intersubband absorption in the sample was measured for the MWIR and LWIR using Fourier transform spectroscopy (FTIR) and the measured peak positions were found at 5.3 μm and 8.7 μm which agree well with the theoretical values obtained 5.0 μm and 9.0 μm for the two infrared bands which indicates the accuracy of the self-consistent model. The photodetectors were fabricated using a standard photolithography process with exposed middle contacts to allow separate bias and readout of signals from the three wavelength bands. The measured photoresponse gave three peaks at 0.84 μm, 5.0 μm and 8.5 μm wavelengths with approximately 0.5 A/W, 0.03 A/W and 0.13 A/W peak responsivities for NIR, MWIR and LWIR bands, respectively. This work demonstrates the possibility of detection of widely separated wavelength bands using interband and intersubband transitions in quantum wells.

Keywords: Infrared detectors; Interband; Intersubband; Quantum wells; Multispectral

1. Introduction

Recent commercial and military applications have demanded photodetectors with high sensitivity, high selectivity and multispectral capability for detection and identification of specific emission signatures [1]. Both mercury cadmium telluride (HgCdTe) photodiodes and quantum well infrared photodetectors (QWIP) offer multicolor capability in the medium-wave IR (MWIR) and long-wave IR (LWIR) spectral regions. Each of these technologies has its advantages and disadvantages, however, the possibility to achieve multicolor detection, going from near infrared (NIR) to LWIR, is more likely to be obtained using QWIPs [2].

Several approaches have been reported about the fabrication of quantum-well infrared photodetectors that includes near-infrared with longer wavelengths sensing capabilities [3]. Those approaches primarily based on the use of intersubband and interband transitions in square quantum wells under high bias to allow interband transitions between bound states with different quantum numbers and yield appreciable responsivity [3–5]. The attempt to use two stacks of quantum wells by Cohen et al. [5] showed some difficulty in controlling the bias across the two stacks due to the

* Corresponding author.
E-mail address: durante@ita.br (F. D. P. Alves).

1350-4495/$ - see front matter © 2006 Elsevier B.V. All rights reserved.
doi:10.1016/j.infrared.2006.10.021

difference in impedance caused by the doped layers. Touse et al. [6] fabricated a dual-band detector using GaAs/InGaAs step quantum wells to improve the interband transition rate and increase the near-infrared responsivity. In their configuration intersubband and interband transitions are detected in the same quantum well restricting the readout flexibility. This article reports the design and fabrication of a QWIP capable to sense simultaneously three different widely separate IR bands including NIR, with separate readouts.

2. Detector design

In the design of the quantum well structure, the quantized energy levels inside the wells as well as their respective wavefunctions were computed self-consistently solving the Schrödinger–Poisson equation numerically. The electron wavefunctions in the heterostructure were computed using the effective mass approximations for the one-dimensional potential profile along the growth direction [7]. The band non-parabolicity effects were incorporated in the model [8] and the strain due to the difference in lattice constants between GaAs or AlGaAs and InGaAs crystal layers [9] was not taken into account. For the valence band, the heavy and light hole bands [8] were represented using average negative effective masses, mhh and mlh, respectively [7]. In this case, the well potential is a confining potential for holes and the same model used for electrons in the conduction band becomes applicable.

The band edge potential was determined by the band offsets between different semiconductor layers [10] and the detector bias is represented by a linear electric field [11]. In addition, high doping concentrations in the quantum well layers can give rise to a significant additional potential on top of the band edge potential [12] due to non-uniform charge distribution. The charge distribution potential was included in our model through a self-consistent approach to compute the overall structure potential. This approach can be summarized as follows. First, the band edge potential is computed from the structure material properties. Then the potential due to applied electric field is computed and added to the band edge potential. The next step is to solve the Schrödinger's equation for the structure, to obtain the bound states and their respective wavefunctions. This is done using the shooting method [12] due to its ability to handle arbitrary potential profiles making the design more flexible. These results will be used as the first guess to compute the charge distribution potential with the help of the Poisson's equation. The charge distribution potential is then added to the previous potential values and the Schrödinger's equation is solved to the new potential. The interactions repeat until the convergence is achieved.

To have the capability to detect simultaneously three different IR bands, including NIR and assuring independent readouts, we employed a configuration with three different stacks of quantum wells formed by alloys of GaAs, AlGaAs and InGaAs, separated by GaAs contact layers. Fig. 1 shows a pictorial view of the device configuration.

The first well stack from the bottom is responsible for detecting the NIR. The shortest wavelength detected using intersubband transitions reported in the literature [13] is about 2.7 μm. Thus, interband transitions are more appropriate for the NIR band. Furthermore, according to the selections rules for interband transitions in quantum wells, the well should be asymmetric to allow the transition from the ground state of the valence band to the first exited state of the conduction band [6]. This is needed to efficiently collect the photoexcited electrons and hence a step well configuration was employed for NIR detection. The middle well stack is responsible for mid-infrared detection. This was accomplished by intersubband transitions in a deep quantum well with AlGaAs barriers and GaAs/InGaAs/GaAs well. The use of GaAs layers in the well reduces the average indium concentration which prevents the strain relaxation. The wells were heavily doped to increase the MWIR absorption.

The stack on the top is responsible for the long-infrared detection. This is the most commonly used configuration and was achieved without much difficulty using shallow wells of AlGaAs/GaAs. The principal constraint here is to control the dark current as a result of thermionic emission [13]; hence the doping concentration was decreased in comparison with the MIWR configuration. Using the model described in the previous section, and the considerations mentioned above, the detector was designed and the final configuration is comprised of 67 semiconductor layers grown by molecular beam epitaxy (MBE) on a GaAs substrate as follows: a 2×10^{18} cm^{-3} Si doped GaAs (0.7 μm) buffer layer; 20 periods of undoped GaAs (300 Å)/$In_{0.10}Ga_{0.90}As$ (43 Å)/$In_{0.25}Ga_{0.75}As$ (40 Å)/GaAs (300 Å) step quantum wells, a 2×10^{18} cm^{-3} Si doped GaAs (0.5 μm) contact layer; 20 periods of $Al_{0.40}Ga_{0.60}As$ (300 Å)/GaAs (13 Å)/$In_{0.15}Ga_{0.85}As$ (14 Å)/GaAs (13 Å)/$Al_{0.40}Ga_{0.60}As$ (300 Å) quantum wells where the three internal layers were 2×10^{18} cm^{-3} Si doped; a 2×10^{18} cm^{-3} Si

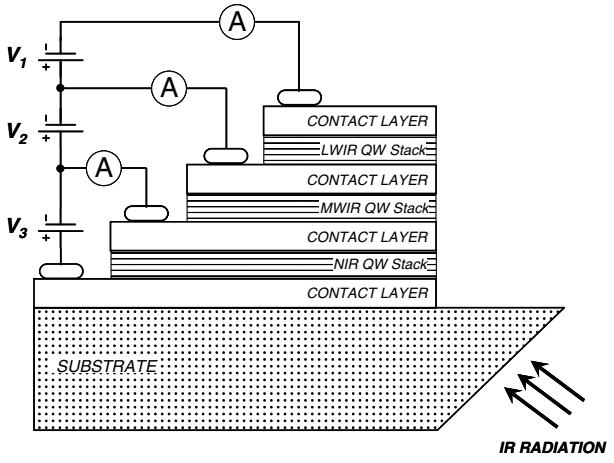

Fig. 1. Schematic diagram of a multi-stack quantum well photodetector with independent readouts.

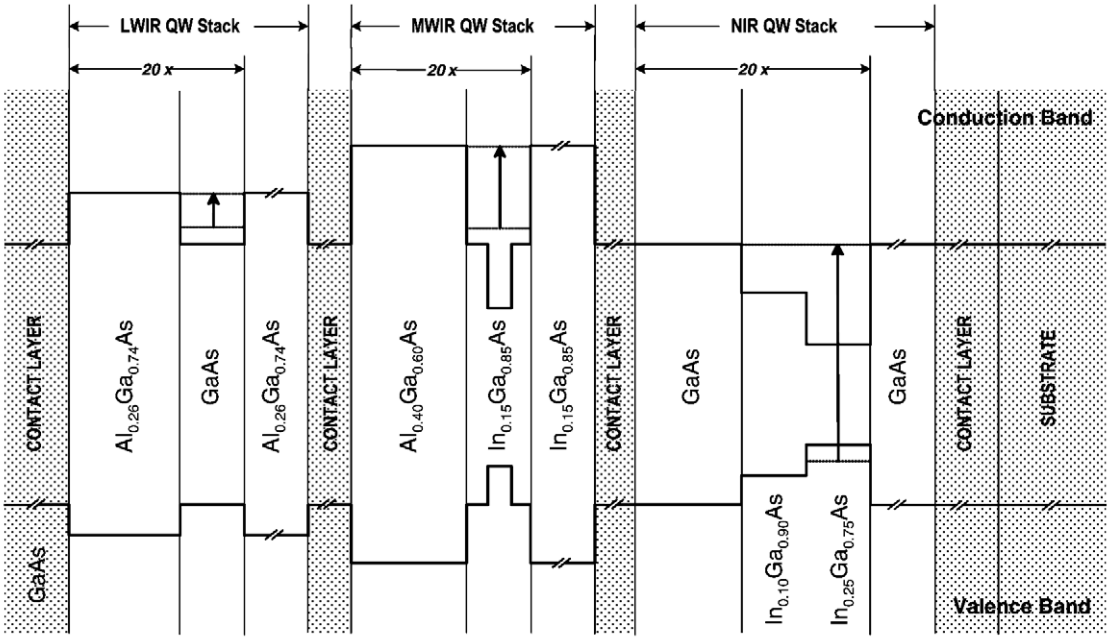

Fig. 2. Band diagram of the GaAs based three color QWIP sample.

doped GaAs (0.5 μm) contact layer; 20 repetitions of $Al_{0.26}Ga_{0.74}As$ (300 Å)/GaAs (52 Å)/$Al_{0.26}Ga_{0.74}As$ (300 Å) quantum wells where the GaAs well was 5×10^{17} cm^{-3} Si doped; and finally a 2×10^{18} cm^{-3} Si doped GaAs (0.7 μm) cap layer. Fig. 2 shows a schematic band diagram of the sample along with the transitions used for detecting the three wavelength bands indicated by the arrows.

The sample was grown on a 3″ diameter semi-insulating GaAs substrate by IQE using molecular beam epitaxy (MBE).

3. Experimental results

Intersubband absorption in the sample was measured for the MWIR and LWIR using Fourier transform spectroscopy (FTIR) using 45° waveguide (4.8 mm long, 13.6 mm wide and 0.66 mm thick) to enhance the absorption. The measured peak positions found at 5.3 μm and 8.7 μm agree well with the calculated values obtained 5.0 μm and 9.0 μm for the two infrared bands. Fig. 3 shows the comparison of the predicted and measured normalized absorption spectra.

In Fig. 3, the dashed curve is the estimated absorption using 300 K material parameters and band offset from [10] as well as the measured spectral broadening parameters. The uncertainties in the estimation of the absorption coefficient are mainly due to the simplifications made in the model and the availability of the semiconductor parameters. However, the estimated peak positions are within 0.3 μm of the measured values, which indicates the model gives good description of the absorption. The FTIR measurement did not cover the NIR region due to the limita-

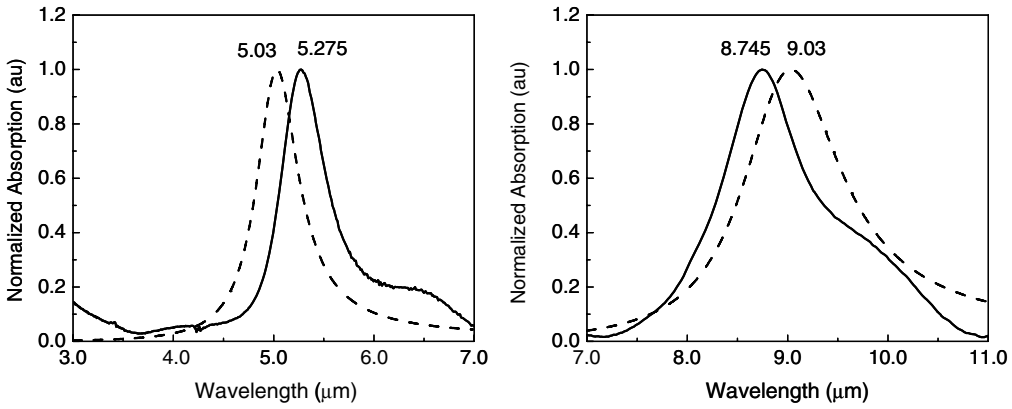

Fig. 3. Comparison between the estimated and the measured MWIR and LWIR normalized absorption spectra.

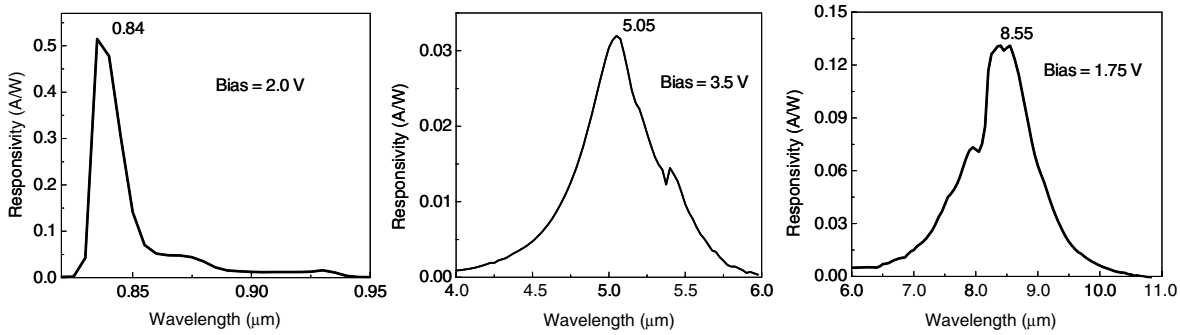

Fig. 4. Measured photocurrent spectra of the detector at 10 K as a function of wavelength in the NIR, MWIR and LWIR regions.

tions of the spectrometer. However, the spectral response in this band can be characterized using photocurrent measurement.

For the photocurrent measurement, devices were fabricated with mesas of $200 \times 200\ \mu m^2$ for the LIWR quantum well stack, $200 \times 400\ \mu m^2$ for the MIWR stack and $200 \times 600\ \mu m^2$ for the NIR with exposed middle contacts to allow separate bias and readout of signals from the three wavelength bands, as schematically shown in Fig. 1.

The spectral responses of the three detectors were measured using a computer-controlled photocurrent spectroscopy system consisting of a multiple-grating monochromator and two light sources to cover the interested wavelength bands. The light was shinned onto the device through a 45° angle facet polished on the wafer to enhance the coupling for the two IR bands based on intersubband transitions. Fig. 4 shows the measured responsivity for all three bands at 10 K using 2.0, 3.5 and 1.75 V biases across the NIR, MIWR and LIWR stacks, respectively.

The observed response in the 0.82–0.95 μm wavelength band is due to interband transitions involving both, LH and HH hole states to the states in the conduction, and is in good agreement with the designed values centered around 0.87 μm in Fig. 2. The fast drop of the photocurrent at about 0.82 μm is due to absorption of incident light by the GaAs substrate. The relatively strong rise at around 0.84 μm is most likely due to the transition between first excited hole and electron states as indicated in Fig. 2. It was found that by increasing the bias, the NIR response became much more uniform within its detection range as shown in Fig. 5 This is possibly due to field ionization of photoexcited electrons in the well which increase the photocurrent and hence the responsivity. The reduction in response near 0.84 μm compared to that in Fig. 4 is probably due to shifting of quasi-bound states to the continuum which reduces the oscillator strength [13].

The responses of the MWIR and LWIR detectors show good agreement with the predicted peak positions. Even though the LWIR quantum wells were doped with a lower Si concentration than the MWIR quantum wells, the high band with peak at 8.55 μm presented higher responsivity (0.13 A/W) than the middle band (0.03 A/W) with peak at 5.05 μm. These observations are consistent with the measured peak absorption strengths of 0.7 Abs and 0.3 Abs for the two transitions, respectively. One possible explanation for the low responsivity for the mid-wave band is that the actual doping density in the well is lower than the designed value. Further study to fully understand this behavior.

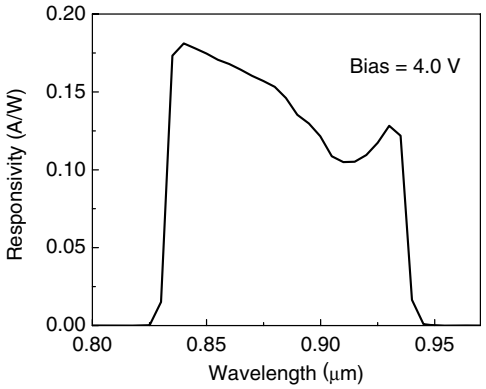

Fig. 5. The measured photocurrent spectra of the detector at 10 K as a function of wavelength in the NIR region with 4 V bias.

4. Conclusions

In summary, a near-, mid- and long-infrared photodetector with separate readouts was fabricated using interband and intersubband transitions in a quantum well structure. The measured absorption and photocurrent data show a good agreement with the self-consistent model develop for the design of the quantum well structure. The photocurrent spectroscopy measurements demonstrate the possibility of detection of widely separated wavelength bands using interband and intersubband transitions in quantum wells. Finally, this approach presents a great potentiality in designing detectors to sense specific emission signatures.

Acknowledgement

The work is supported in part by a grant through the Research Office of the Naval Postgraduate School.

References

[1] D.C. Schleher, Electronic Warfare in the Information Age, Artech House, Norwood, MA, 1999, pp. 429–468.
[2] A. Rogalski, Infrared Phys. Technol. 38 (1997) 295.
[3] H.C. Liu, C.Y. Song, E. Dupont, P. Poole, P.H. Wilson, B.J. Robinson, D.A. Thonpson, Electron. Lett. 14 (1993) 566.
[4] H.C. Liu, C.Y. Song, A. Shen, M. Gao, Z.R. Wasilewski, M. Buchanan, Appl. Phys. Lett. 77 (2000) 2437.
[5] N. Cohen, A. Zussman, G. Sarusi, Infrared Phys. Technol. 42 (2001) 391.
[6] M.P. Touse, G. Karunasiri, K.R. Lantz, H. Li, T. Mei, Appl. Phys. Lett. 86 (2005) 093501/1.
[7] E. Rosencher, B. Vinter, Optoelectronics, Cambridge University Press, London, 2002, pp. 344–350.
[8] M.O. Manasreh, Semiconductor Quantum Wells and Superlattices for Long-Wavelength Infrared Detectors, Artech House, Inc., Norwood, MA, 1993, pp. 28–31.
[9] H.C. Chui, S.M. Lord, E. Marinet, M.M. Fejer, J.S. Harris Jr., Appl. Phys. Lett. 63 (1993) 364.
[10] I. Vurgaftman, J.R. Meyer, J. Appl. Phys. 89 (2001) 5815.
[11] F.Y. Huang, J. Li, Lie-Ming Li, H. Morcoc, Appl. Phys. Lett. 63 (1993) 1669.
[12] P. Harrison, Quantum Wells, Wires and Dots: Theoretical and Computational Physics, John Wiley & Sons Inc., New York, 2001, pp. 23–30.
[13] B.F. Levine, J. Appl. Phys. 74 (1993) 1.